

Wetting of a particle in a thin film

Jennifer Fiegel^{a,1}, Fang Jin^a, Justin Hanes^{a,b}, Kathleen Stebe^{a,b,c,d,*}

^a Department of Chemical & Biomolecular Engineering, Johns Hopkins University, Baltimore, MD 21218, USA

^b Department of Biomedical Engineering, Johns Hopkins University, Baltimore, MD 21218, USA

^c Department of Materials Science & Engineering, Johns Hopkins University, Baltimore, MD 21218, USA

^d Department of Mechanical Engineering, Johns Hopkins University, Baltimore, MD 21218, USA

Received 11 January 2005; accepted 7 May 2005

Available online 8 June 2005

Abstract

When a particle is placed in a thin liquid film on a planar substrate, the liquid either climbs or descends the particle surface to satisfy its wetting boundary condition. Analytical solutions for the film shape, the degree of particle immersion, and the downward force exerted by the wetting meniscus on the particle are presented in the limit of small Bond number. When line tension is significant, multiple solutions for the equilibrium meniscus position emerge. When the substrate is unyielding, a dewetting transition is predicted; that is, it is energetically favorable for the particle to rest on top of the film rather than remain immersed in it. If the substrate can bend, the energy to drive this bending is found in the limits of slow or rapid solid deflection. These results are significant in a wide array of disciplines, including controlled delivery of drugs to pulmonary airways, the probing of liquid film/particle interface properties using particles affixed to AFM tips and the positioning of small particles in thin films to create patterned media.

© 2005 Elsevier Inc. All rights reserved.

1. Introduction

A particle will enrobe itself in a fluid until its contact angle boundary condition is satisfied. The partial wetting of particles has been extensively studied because of its importance in several applications, including froth flotation as a means of recovering ore particles [1–3], the use of partially wetted particles to form or disrupt emulsions [4,5], the use of aerosol particles laden with drugs in particle-based drug delivery [6,7], and, more recently, the use of evaporating thin films containing particles to create colloidal crystals [8].

The configuration of spherical particles and their pairwise interaction at interfaces of infinitely deep fluids has been extensively studied cf. [1–5,9–13]. The weight or buoyancy of the particles deflects the surfaces, which bend over distances comparable to the capillary length. Asymmetric

menisci form when particles are closer than the capillary length, creating net forces between particles that drive them toward each other. For small Bond number Bo (the ratio of gravitational forces to surface tension forces on the particle), the fluid interface becomes planar, and capillary interactions between particles vanish [11].

The situation of a single particle in a thin film has been less studied. For the case of two free surfaces, spherical particles spanning the film have been used to infer film heights in a film-thinning apparatus by comparing the shape of the interface inferred by interference fringes to the shape predicted by integrating the Young–Laplace equation [14]. In contrast, pairs of particles in a thin liquid film [8,15–18] have been extensively studied to understand attractive interactions caused by the menisci between them. Even in the limit of vanishing Bo , these interactions remain finite when the film thickness is less than the particle diameter. These forces are exploited in techniques to create colloidal assemblies.

In this work, an analysis of the wetting of a single particle in a thin fluid film on top of a planar surface is presented. In the small slope limit, analytical solutions for the inter-

* Corresponding author. Fax: +1 (410) 516 5510.

E-mail address: kjs@jhu.edu (K. Stebe).

¹ Current address: Division of Engineering and Applied Sciences, Harvard University, Cambridge, MA 02138, USA.

face shape, the degree of submersion of the particle and the magnitude of the forces on the underlying solid surface are derived. The effects of line tension are also considered. Depending on its sign, line tension can either further submerge or float particles. A discontinuous dewetting transition is predicted for critical values of the (positive) line tension. That is, for large enough line tensions, it is energetically favorable for the particle to rest on top of the film rather than to immerse itself in it. This transition is discussed in comparison to the discontinuous wetting transition predicted for particles at interfaces of deep fluids [12].

The wetting meniscus exerts a downward force on the particle. To estimate whether the particle can bend the underlying substrate, an energy analysis is performed in the limits of slow or rapid substrate bending. Such substrate deflection has been reported for small particles placed in thin liquid films in the lung [6]. A brief discussion of the implications of these results in that context is presented.

2. Theory

2.1. Force balance on the particle

A spherical particle of radius a placed on a planar support covered with a thin liquid film of far-field thickness $h_\infty < 2a$ will enrobe itself in liquid to satisfy its contact angle θ to form a wetting angle ϕ_c (which locates the 3-phase contact line) as shown in Fig. 1. A vertical force balance on the particle yields:

$$\frac{4}{3}\pi a^3 g \left\{ (\rho_s - \rho_v) - \frac{(\rho_L - \rho_v)}{4} \left[2 - 3 \cos \phi_c + \cos^3 \phi_c - 3 \frac{(h_c - h_\infty)}{a} \sin^2 \phi_c \right] \right\} + 2\pi a \gamma \sin \phi_c \sin(\phi_c + \theta) - F_N = 0, \quad (1)$$

where ρ_i ($i = s, L, v$) denote densities, with subscript s , L and v referring to the solid particle, the liquid film and the surrounding vapor phases, respectively, and γ denotes the surface tension. In Eq. (1), the first term contains the forces exerted by gravity on the particle (including buoyant forces exerted by the fluid which intersects the sphere at height $h_c = a(1 - \cos \phi_c)$); the second term is the surface tension force exerted along the wetted perimeter (of length $2\pi a \sin \phi_c$); and the third term F_N is the magnitude of the upward normal force exerted by the underlying solid on the particle at the wetted pole. This equation can be recast in non-dimensional form to become:

$$\frac{4}{3}\pi Bo \left[\frac{\rho_s - \rho_v}{\rho_L - \rho_v} - \frac{1}{4} \left[2 - 3 \cos \phi_c + \cos^3 \phi_c - 3 \frac{(h_c - h_\infty)}{a} \sin^2 \phi_c \right] \right]$$

$$- 2\pi \sin \phi_c \sin(\phi_c + \theta) + \frac{F_N}{a\gamma} = 0, \quad (2a)$$

where Bo , the Bond number, is defined:

$$Bo = \frac{(\rho_L - \rho_v)ga^2}{\gamma}. \quad (2b)$$

For significant Bond numbers, the gravitational terms must be retained, as discussed in detail in references [1] and [10]. However, for solid particles with radii less than millimeters in aqueous systems, $Bo \ll 1$. Provided that Bo and the product $Bo[(\rho_s - \rho_v)/(\rho_L - \rho_v)]$ are small, the first term in Eq. (2a) can be neglected, and the force balance becomes:

$$\frac{F_N}{a\gamma} = 2\pi \sin \phi_c \sin(\phi_c + \theta). \quad (2c)$$

Equation (2c) requires that F_N be as large as necessary to balance the surface tension wetting force. Note that if h_∞ were greater than $2a$, F_N would be zero, so the net vertical surface tension force would also be zero requiring $180^\circ = \theta + \phi_c$ for all θ , recovering the known solution of a flat interface for large film thicknesses ($h_\infty > 2a$).

2.2. The film interface shape

The shape of the fluid interface is determined by the Young–Laplace equation in cylindrical coordinates:

$$(\rho_v - \rho_L)g(h(r) - h_\infty) = - \left[\frac{h''}{(1 + (h')^2)^{3/2}} + \frac{1}{r} \frac{h'}{\sqrt{1 + (h')^2}} \right] \gamma, \quad (3)$$

where the primes indicate derivatives of h with respect to the radial coordinate. For small Bo , $(h')^2 \ll 1$, so Eq. (3) can be simplified by approximating the denominators on the right-hand side as unity. The equation is then recast in dimensionless form according to:

$$G(\hat{r}) = \frac{h(r) - h_\infty}{a}, \quad \hat{r} = \frac{r}{L_c}, \quad \hat{h} = \frac{r}{a}, \quad (4a)$$

where L_c is a capillary length, defined as:

$$L_c = \sqrt{\frac{\gamma}{\Delta\rho g}} \quad (4b)$$

to yield a modified Bessel equation:

$$G'' + \frac{G'}{\hat{r}} - G = 0 \quad (5)$$

subject to two boundary conditions:

$$\lim_{\hat{r} \rightarrow \infty} G = 0, \quad (6a)$$

$$G(\hat{r} = \sin \phi_c \sqrt{Bo}) = \hat{h}_c - \hat{h}_\infty. \quad (6b)$$

Thus, the final expression for the shape of the liquid–gas interface is:

$$\hat{h}(\hat{r}) = \hat{h}_\infty + \frac{\hat{h}_c - \hat{h}_\infty}{K_0(\sin \phi_c \sqrt{Bo})} K_0(\hat{r}), \quad (7)$$

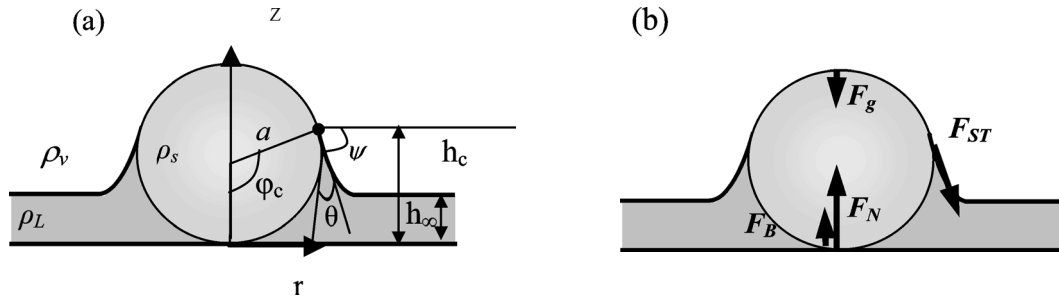


Fig. 1. (a) Particle of radius a and density ρ_s situated in a thin liquid film of thickness h_∞ and density ρ_L on a planar substrate. A vapor phase of density ρ_v is above the liquid. To satisfy the contact angle θ , the fluid climbs the particle to a height h_c with a wetting angle ϕ_c at the contact line. (b) Forces acting on a particle situated in a thin film of liquid. F_g is the particle weight; F_B is the buoyant force; F_{ST} is the force exerted by the meniscus and F_N is the normal reaction force exerted by the substrate on the particle.

where $\hat{h}_c = 1 - \cos \phi_c$ and K_0 denotes the modified Bessel function of order zero.

The slope of Eq. (7) can be used to find $\tan \psi \sim \psi$, the angle made by the interface with the horizontal.

$$\begin{aligned} \psi &= -\sqrt{Bo} \frac{d\hat{h}}{d\hat{r}} \Big|_{\sqrt{Bo} \sin \phi_c} \\ &= \frac{\sqrt{Bo}(\hat{h}_c - \hat{h}_\infty)}{K_0(\sqrt{Bo} \sin \phi_c)} K_1(\sqrt{Bo} \sin \phi_c), \end{aligned} \quad (8)$$

where K_1 denotes the modified Bessel function of order one. The angle ψ can be related to the contact angle by:

$$\psi = 180 - \phi_c - \theta. \quad (9)$$

Combining Eqs. (8) and (9):

$$\phi_c = 180 - \theta - \frac{\sqrt{Bo}(\hat{h}_c - \hat{h}_\infty)}{K_0(\sqrt{Bo} \sin \phi_c)} K_1(\sqrt{Bo} \sin \phi_c). \quad (10)$$

In principle, Eq. (10) allows us to find the degree of immersion of a particle in a thin film as a function of the contact angle θ , the Bond number Bo , and the far-field film thickness, \hat{h}_∞ , all of which would be known quantities in an experiment. However, because Eq. (10) is a transcendental equation, solving for ϕ_c given θ , Bo and \hat{h}_∞ is not convenient. It is convenient to specify Bo , ϕ_c , \hat{h}_∞ and solve afterwards for the contact angle θ consistent with those parameters and slopes using Eq. (10). Thereafter, F_N can be determined from Eq. (2c). In performing these calculations, polynomial expansions are used to approximate the modified Bessel functions, K_0 and K_1 [19]. (Alternatively, simple asymptotic approximations in the limit of small argument x could be adopted, for which $K_0(x) = -C + \ln(x/2)[1 + O(x^2/4)]$, $K_1(x) = 1/x + O((x/2) \ln(x/2))$.)

2.3. Line tension

For large wetting peripheries, line tension effects are typically negligible, and the analysis given above suffices to describe a particle in a thin film. However, for smaller particle radii, line tension can become important. In the absence

of line tension, mechanical equilibrium at the 3-phase contact line requires that the Young equation be satisfied:

$$\cos \theta_0 = \frac{\gamma_{sv} - \gamma_{sL}}{\gamma}, \quad (11)$$

where γ_i ($i = sv, sL$) is the interfacial energy of the solid surface, with subscripts sv and sL referring to the solid–vapor and solid–liquid interfaces respectively, and γ is the surface tension of the liquid–vapor interface introduced in Eq. (1). In Eq. (11), the contact angle θ_0 is introduced to refer to the contact angle when line tension effects are negligible.

Let Σ denote a dimensionless line tension,

$$\Sigma = \frac{\sigma}{\gamma a}, \quad (12)$$

where σ is the line tension. When line tension is important, the modified Young equation governs the contact angle [20]:

$$\cos \theta = \cos \theta_0 - \Sigma \cot \phi_c, \quad (13)$$

where θ is the contact angle including the effects of line tension, which differs from θ_0 for fixed σ for particles with small radii. (One can imagine measuring θ_0 on very large particles made of the material of interest. The line tension σ is fixed by intermolecular interactions along the three-phase contact line. Thus, θ_0 and σ can be treated as the material parameters in the problem. However, the mechanical response of the system is determined by θ , defined in Eq. (13), which indeed reduces to θ_0 when Σ is negligible.)

Inserting the expression for θ from Eqs. (10) into (13) gives:

$$\begin{aligned} \Sigma &= \frac{\cos \theta_0}{\cot \phi_c} + \cos \left[(\phi_c + \sqrt{Bo}(\hat{h}_c - \hat{h}_\infty)) \right. \\ &\quad \left. \times \frac{K_1(\sqrt{Bo} \sin \phi_c)}{K_0(\sqrt{Bo} \sin \phi_c)} \right] \frac{1}{\cot \phi_c}. \end{aligned} \quad (14)$$

Equation (14) provides an implicit relationship for the effect of line tension on modifying the contact line position ϕ_c .

3. Results and discussion

3.1. Interface shape and forces exerted on the substrate

Fig. 2a shows the interface shape $\hat{h}(\hat{r})$ for $Bo = 10^{-6}$ and $\hat{h}_\infty = 0.3$ for several values of the contact angle θ . This figure also captures the dependence of the interface shape on the Bond number Bo implicitly in that the radial coordinate is scaled by the capillary length L_c so that; $\hat{r} = r/L_c = (r/a)\sqrt{Bo}$. Increasing Bo decreases the length scale L_c over which the meniscus approaches its planar asymptote. For small Bo , a particle deflects the interface over distances orders of magnitude larger than the particle itself. The effects of varying the contact angle are also reported in Fig. 2. The interface intersects the particle with a planar surface for $\theta = 135^\circ$. To satisfy contact angles lower than that value, the interface deflects upwards (e.g., for $\theta = 45$, the fluid climbs the sphere to establish a contact line positioned at $\phi_c = 123.4$); for contact angles greater than this value, it bends downwards (e.g., for $\theta = 180$, the meniscus descends along the sphere to locate the contact angle at $\phi_c = 10.3$). In Fig. 2b, the interface shape close to the particle is shown. In this case, both axial and radial coordinates are scaled with the particle radius a .

In Fig. 3, the angle defining the degree of submersion of the particle ϕ_c is plotted as a function of θ for various values of \hat{h}_∞ . Consider the behavior at some fixed value of θ . If $\hat{h}_\infty = \hat{h}_{\infty\text{flat}} = 1 + \cos\theta$, the film intersects the particle

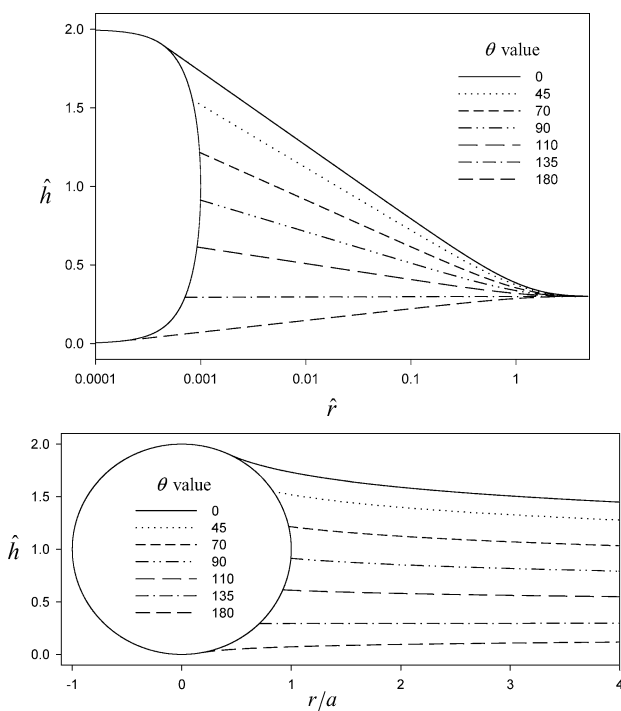


Fig. 2. The interface shape for a particle in a film with $\hat{h}_\infty = 0.3$ and $Bo = 1 \times 10^{-6}$ for various values of θ . (a) \hat{h} is scaled with the particle radius, \hat{r} is scaled with L_c . (b) Close-up of interfaces near particle surface; both axes are scaled with the particle radius.

with a planar interface so that θ is satisfied. Then, the interface does not deflect, and $\phi_{c\text{flat}} = 180^\circ - \theta$. For thinner films, the interface must bend upward to satisfy its contact angle boundary condition (i.e., $\psi > 0$), so ϕ_c decreases. It is interesting to note that perfect wetting of a particle cannot be achieved for film thickness less than the particle diameter. Even when $\theta = 0$, there is a maximum value for $\phi_{c\text{Max}}$ that is less than π . This bound occurs because for $\hat{h}_\infty < 2$, the interface must bend to wet the particle, so $\psi > 0$. Since $\theta + \phi_c + \psi = 180^\circ$, the maximum wetting angle $\phi_{c\text{Max}}$ is determined by $\phi_{c\text{Max}} = 180^\circ - \psi(\phi_{c\text{Max}}, \hat{h}_\infty, Bo)$. This implicit equation for $\phi_{c\text{Max}}$ defines the intercepts in Fig. 3 at $\theta = 0$. Similarly, when $\theta = 180^\circ$, there is no finite thickness for the film for which ϕ_c is zero; in order to try to dewet the sphere, the interface deflects downward, and $\psi < 0$. Thus, there is a minimum value for ϕ_c defined by $\phi_{c\text{Min}} = -\psi(\phi_{c\text{Min}}, \hat{h}_\infty)$, defining the values for ϕ_c in Fig. 3 at $\theta = 180^\circ$.

In Fig. 4a, the force F_N is shown as a function of contact angle θ for various \hat{h}_∞ . The greater the deflection of the interface, the greater is the magnitude of the force. For the case where the interface remains perfectly planar (i.e., $\hat{h}_\infty = \hat{h}_{\infty\text{flat}}$), F_N is zero. For $\hat{h}_\infty < \hat{h}_{\infty\text{flat}}$, the wetting meniscus pulls the particle down onto the surface and $F_N > 0$. For cases $\hat{h}_\infty > \hat{h}_{\infty\text{flat}}$, the non-wetting meniscus pulls the particle away from the solid. This configuration is only possible if the solid exerts a downward, attractive force $F_N < 0$. In Fig. 4b, the magnitude of F_N is shown to increase with Bo for $\hat{h}_\infty = 0.3$, since the greater is Bo , the greater is the surface deflection.

3.2. Line tension effects

Line tension can change the equilibrium wetting configuration significantly. In order to place our results in context, the behavior of a sphere in a deep fluid studied in detail by Aveyard and Clint [12] is briefly described. For this case, the interface must remain planar for the force balance to be satisfied, so $\phi_c = 180^\circ - \theta$. Solving Eq. (13) for θ as a

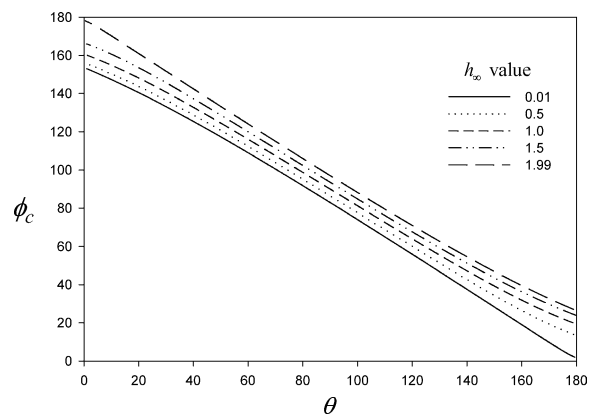


Fig. 3. Angle of intersection with particle ϕ_c as a function of contact angle θ for various \hat{h}_∞ for fixed $Bo = 1 \times 10^{-6}$. ϕ_c depends only weakly on \hat{h}_∞ because of small Bo .

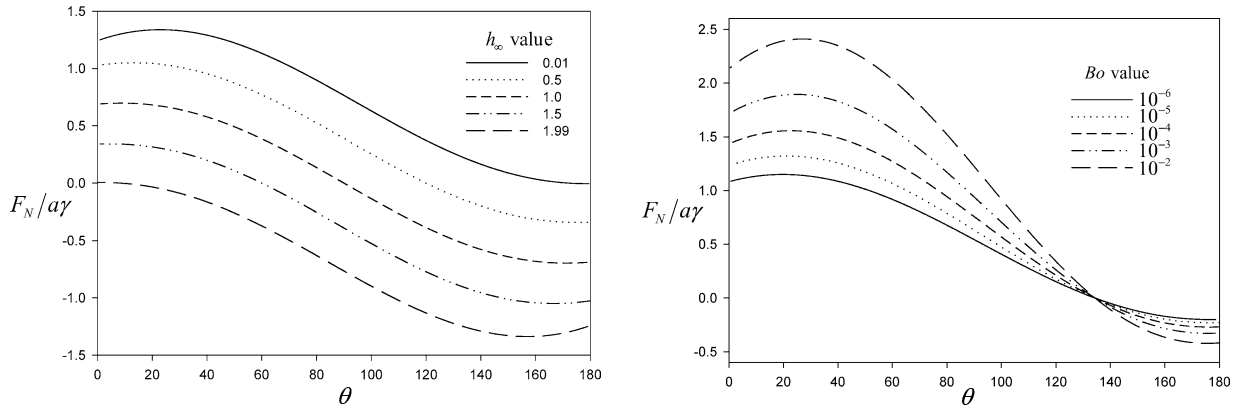


Fig. 4. (a) Forces F_N exerted by solid surface on particle as a function of contact angle θ for various \hat{h}_∞ for fixed $Bo = 1 \times 10^{-6}$. (b) F_N as a function of contact angle θ for various Bo for fixed $\hat{h}_\infty = 0.3$.

function of Σ for fixed $\theta_0 = 70^\circ$ yields the results shown in Fig. 5a. Over an extended range of Σ , there are multiple solutions for θ ; the continuous loop for θ shown in the lower left-hand side of the graph, and another branch of solutions shown above that loop which becomes the sole solution at large Σ . There is another possible configuration for a particle in a deep fluid: it can undergo a wetting transition and be pulled under the liquid surface. An energy analysis can be used to ascertain which of these solutions are stable. The stable configurations, described in detail in [12], are shown as the bold lines in Fig. 5a. As Σ increases, the contact line reduces slightly (i.e., θ decreases). At a critical value for the line tension Σ_{wet} the particle abruptly undergoes a wetting transition. (While these authors did not comment on the upper branch of solutions in their study, their results remain unaltered, since the upper branch is not stable when compared to the immersed particle.)

In contrast, a particle situated in a thin film on a solid support that remains planar cannot immerse itself completely in the fluid. This situation is considered in Fig. 5b. The solid lines correspond to $\hat{h}_\infty = 0.1$, $\theta_0 = 70^\circ$, and the dashed curves are simply the results in Fig. 5a, repeated for comparison. Equation (14) yields multiple solutions for θ as a function of Σ , which differ from the deep fluid case because of the finite slope of the interface ψ . While the particle cannot be immersed beneath the film, it can be expelled from it. Thus, another possible configuration is a particle resting on top of the film. (The energy of the point of contact of the sphere on the plane is neglected.) An energy analysis is constructed to ascertain which configuration is stable. At constant T and P , the Helmholtz free energy \mathbf{A}^* of a partially wetted particle in a thin film can be calculated as:

$$\mathbf{A}^* = \gamma_{sL}A_{sL} + \gamma_{sv}A_{sv} + \gamma A_{LV} + 2\pi a \sin \varphi_c \sigma \quad (15)$$

in dimensional form. (In Eq. (15), all terms associated with the gravitational potential energy have been neglected in the limit of small Bo .) The areas of the various interfaces are represented by A_i ($i = sL, sv, LV$). If the location of the contact line changes from φ_{c1} to φ_{c2} , the change in energy can be

calculated as:

$$\begin{aligned} \Delta \mathbf{A}^* &= \mathbf{A}^*(\varphi_{c2}) - \mathbf{A}^*(\varphi_{c1}) \\ &= (\gamma_{sL} - \gamma_{sv})\Delta A_{sL} + \gamma \Delta A_{LV} \\ &\quad + 2\pi a \sigma (\sin \varphi_{c2} - \sin \varphi_{c1}), \end{aligned} \quad (16)$$

where ΔA_{sL} is the change in wetted surface area of the sphere:

$$\Delta A_{sL} = 2\pi a^2 (\cos \varphi_{c1} - \cos \varphi_{c2}), \quad (17)$$

and ΔA_{LV} is the change in area of the liquid–vapor interface, which is given by:

$$\Delta A_{LV} = 2\pi \int_{a \sin \varphi_{c1}}^{a \sin \varphi_{c2}} \left\{ 1 + \left(\frac{dh}{dr} \right)^2 \right\}^{1/2} r' dr' \quad (18a)$$

which in the limit of small Bo becomes:

$$\Delta A_{LV} \approx \pi a^2 [\sin^2 \varphi_{c1} - \sin^2 \varphi_{c2}]. \quad (18b)$$

Inserting these statements into Eq. (16) and rearranging yields:

$$\begin{aligned} \Delta \alpha &= \frac{\Delta \mathbf{A}^*}{\pi a^2 \gamma} \\ &= -2 \cos \theta_{\Sigma=0} (\cos \varphi_{c1} - \cos \varphi_{c2}) \\ &\quad + [\sin^2 \varphi_{c1} - \sin^2 \varphi_{c2}] + 2\Sigma [\sin \varphi_{c2} - \sin \varphi_{c1}]. \end{aligned} \quad (19)$$

If $\Delta \alpha$ is negative, the change in contact line position from φ_{c1} to φ_{c2} decreases the free energy, and so is favored.

Comparing the various solutions, the stable configurations are indicated by the bold lines in Fig. 5b. As Σ increases from zero, θ first decreases slightly, then jumps to zero (which, recall, does not correspond to particle immersion, but rather to $\varphi_{c\text{Max}} = 148.3^\circ$). Thereafter, θ increases until a critical value Σ_{dewet} , for which the particle is expelled from the film in a dewetting transition. Note that this dewetting transition is predicted for a system that favors wetting in the absence of line tension. In Fig. 5c, the corresponding graph of stable φ_c is shown. This behavior is typical for $\theta_0 < 85^\circ$. For larger values, the continuous loop of solutions

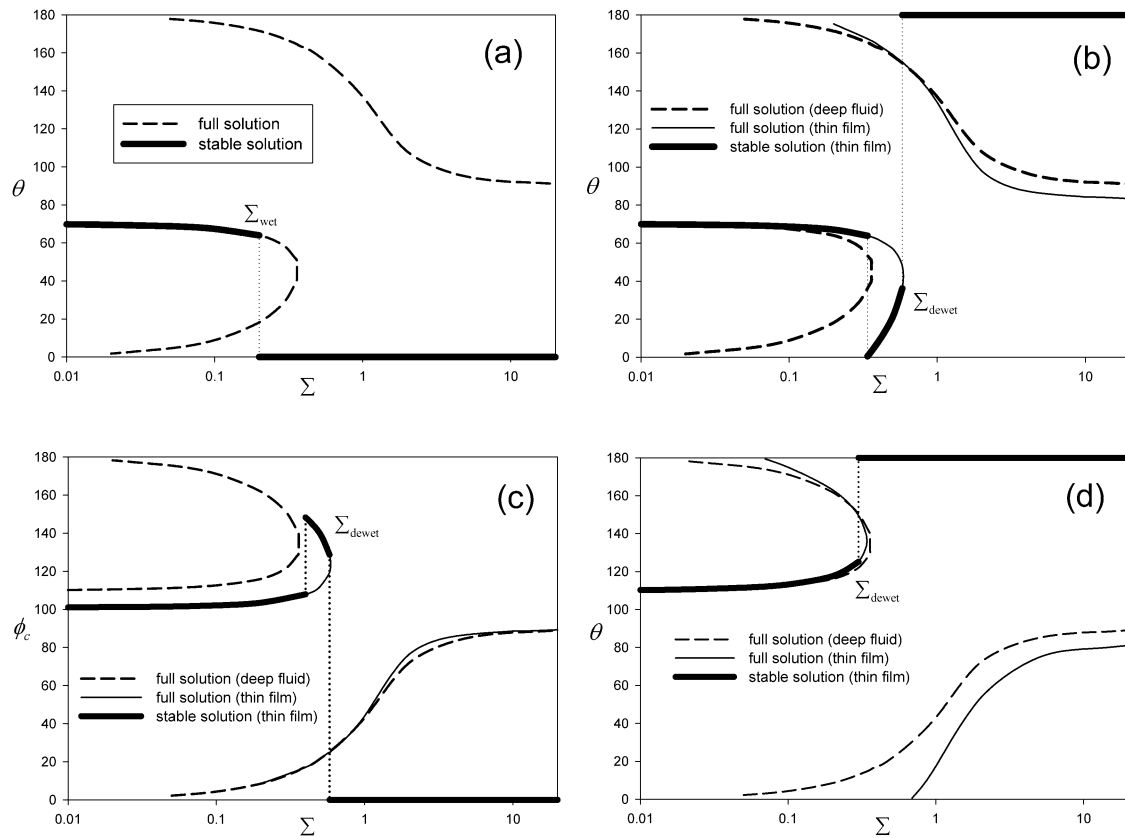


Fig. 5. (a). Contact angle θ as a function of line tension Σ for $\theta_0 = 70^\circ$ for a particle in a deep fluid (valid for $\hat{h}_\infty > 2.0$). Stable solutions are shown by the bold solid line. The critical value for line tension for wetting is Σ_{wet} . (b) Solid curves: contact angle θ as a function of line tension Σ for $\theta_0 = 70^\circ$ for a particle in thin film with $\hat{h}_\infty = 0.1$. Dashed curves: results in Fig. 5a, repeated for comparison. Bold curves: stable solutions. The critical value for line tension for dewetting is Σ_{dewet} . (c) Stable ϕ_c for $\theta_0 = 70^\circ$ for a particle in thin film with $\hat{h}_\infty = 0.1$. (d) Contact angle θ as a function of line tension Σ for $\theta_0 = 110^\circ$. Dashed curve: a particle in a planar interface (valid for $\hat{h}_\infty > 2.0$). Solid curve: a particle in thin film with $\hat{h}_\infty = 0.1$. Bold curves: stable solutions.

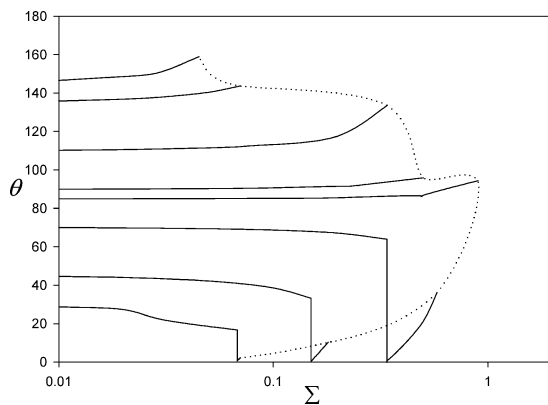


Fig. 6. A graph summarizing the stable contact angle θ as a function of line tension Σ for various θ_0 (the intercept for each curve) for fixed $\hat{h}_\infty = 0.1$. Each curve terminates at Σ_{dewet} . Dashed curve: the envelope of Σ_{dewet} as a function of θ_0 .

is inverted. Stable solutions for θ follow the lowest branch of the curve, and jump to the dewetting transition at a critical value for Σ , as shown in Fig. 5d.

A graph summarizing the stable contact angle solutions θ vs Σ as a function of θ_0 (the intercept on the vertical axis for each curve) for $\hat{h}_\infty = 0.1$ is shown in Fig. 6. Each curve

terminates at the dewetting transition. The dashed curve indicates the envelope Σ_{dewet} values for this transition.

3.3. Flexible substrate

The preceding analysis can lend some insight into the more complex problem in which the substrate on which the particle rests is flexible and is subject to bending by the particle. The force exerted by the particle on the solid surface is $-F_N$, determined by the analysis described above for a given free surface configuration. The energy made available by wetting the particle to deflect the substrate can also be estimated. In making this estimate, the ability of the substrate to exert a restoring force is neglected. Amendments to the analysis to include these effects are straightforward. Two limits for substrate deflection are considered below for the case of a particle placed in a thin film of a given thickness with a given contact angle.

3.3.1. Slow substrate deflection

Consider a particle placed on a thin film with $\hat{h}_\infty = 0.1$ and $\theta = 70$ in the absence of line tension. If the solid surface deflects slowly compared to the rate at which the meniscus adjusts itself to maintain an equilibrium configuration, the

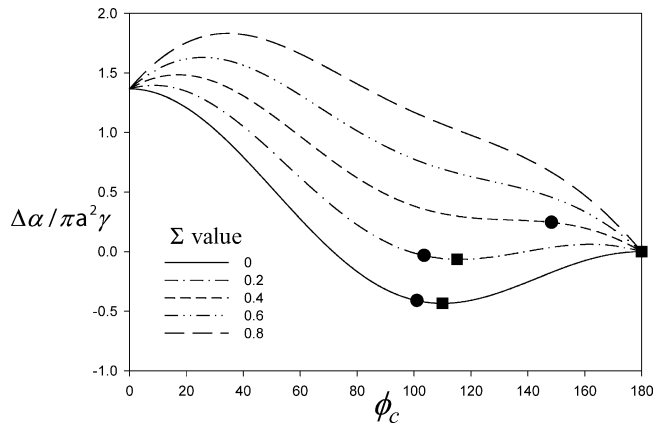


Fig. 7. Energy profile $\Delta\alpha(180^\circ, \phi_c) = \alpha(\phi_c = 180^\circ) - \alpha(\phi_c)$ as a function of Σ for fixed $\theta_0 = 70^\circ$ and $\hat{h}_\infty = 0.1$. For $\Sigma = 0$, $\Delta\alpha = -0.025$, the difference between the circle and square of the $\Sigma = 0$ curve. Recall $\Sigma_{\text{wet}} = 0.25$ and $\Sigma_{\text{dewet}} = 0.58$. Case (i): circle on $\Sigma = 0.2$ ($\Sigma < \Sigma_{\text{wet}}$) curve: $\theta = 67.1^\circ$ and $\phi_c = 103.5^\circ$. Square: a planar interface intersecting the particle with $\theta = 64.2^\circ$ and $\phi_c = 115.8^\circ$. Case (ii): $\Sigma = 0.4$ ($\Sigma_{\text{wet}} < \Sigma < \Sigma_{\text{dewet}}$) circle: $\theta = 8.2^\circ$, $\phi_c = 148.3^\circ$. Case (iii): $\Sigma = 0.6$ ($\Sigma > \Sigma_{\text{dewet}}$) initial state: $\phi_c = 0^\circ$ on the $\Sigma = 0.6$ curve. Final state: $\phi_c = 180^\circ$. The activation energy barrier is given by the difference between the maximum in the free energy and the initial state.

initial state will be that of a particle with a fluid interface configuration in equilibrium with a film of far-field thickness $\hat{h}_\infty = 0.1$. In the final state, the particle will be immersed to a depth dx on the axis of revolution so that the fluid interface is flat, and $F_N = 0$ (i.e., $\hat{h}_\infty + dx = 1 + \cos\theta = 1.34$ and $\phi_c = 110^\circ$ for the example discussed here). Using Eq. (19) to calculate the change of energy in these two states, $\Delta\alpha = -0.025$, indicating energy in the amount $0.025\pi\gamma a^2$ is made available to deflect the substrate.

Line tension effects can be included. Consider the case of $\theta_0 = 70^\circ$, $\hat{h}_\infty = 0.1$, and refer to the energy profile $\Delta\alpha(\pi, \phi_c) = \alpha(\phi_c = \pi) - \alpha(\phi_c)$ reported in Fig. 7. Recall that for $\theta_0 = 70^\circ$, $\Sigma_{\text{wet}} = 0.25$ and $\Sigma_{\text{dewet}} = 0.58$. Three cases must be considered, discussed individually below.

- (i) Consider $\Sigma = 0.2$, for which $\Sigma < \Sigma_{\text{wet}}$. The particle rests initially in a thin film of thickness $\hat{h}_\infty = 0.1$, $\theta = 67.1^\circ$ and $\phi_c = 103.5^\circ$, indicated by a circle on the curve in Fig. 7. (These values correspond to a stable solution of Eqs. (13) and (14), as shown in Fig. 5b and 5c). The final state on a planar fluid interface requires $\theta = 63.9^\circ$ and $\phi_c = 116.1^\circ$, indicated by the square on the curve. (These values correspond to a solution of modified Young equation for θ , and the assumption of a planar interface for ϕ_c .) The change in energy between these two states is $\Delta\alpha = -0.024$. Since the energy decreases monotonically between the initial and final states, there is no energy barrier to this process. If the energy liberated by immersing the particle is sufficient to bend the underlying substrate, it will spontaneously do so.
- (ii) Consider $\Sigma = 0.4$, for which $\Sigma_{\text{wet}} < \Sigma < \Sigma_{\text{dewet}}$. For this case, the initial state consists of a particle in a thin

film in equilibrium with this value of Σ (i.e., $\theta = 8.2^\circ$, $\phi_c = 148.3^\circ$, indicated by a circle on the curve in Fig. 7), while the final state corresponds to a completely immersed particle ($\phi_c = 180^\circ$). The energy liberated in immersing the particle is $\Delta\alpha = -0.246$, with no activation energy barrier to this immersion being provided by the particle.

- (iii) Consider $\Sigma = 0.6$, for which $\Sigma > \Sigma_{\text{dewet}}$. For this case, the initial state consists of a particle that has been expelled from the thin film (corresponding to $\phi_c = 0^\circ$ on the $\Sigma = 0.6$ curve in Fig. 7), while the final state consists of a particle submerged in the fluid (corresponding to $\phi_c = 180^\circ$ on the same curve). The energy difference between the final and initial states is $\Delta\alpha = -1.31$. The free energy activation energy barrier between these states is evident in Fig. 7. The free energy first increases as ϕ_c increases from zero, then decreases. The height of the maximum in free energy above the initial state defines the activation free energy barrier $\Delta E_{\text{act}} = 0.265$. (This can be understood in approximate terms by considering the transient state in which a hole is created in the liquid–vapor interface (with a free energy decrease of -1 in scaled form) while the perimeter of that hole increases the free energy by 2Σ (with a free energy increase of 1.2), thus creating an energy barrier of roughly 0.2 .) For all $\Sigma > \Sigma_{\text{dewet}}$, the initial and final states remain the same as those described in the case above. The energy liberated by immersing the particle increases linearly with $\cos\theta_0$, and the activation energy barrier increases linearly with Σ , as the cost of the transient state increases.

3.3.2. Rapid substrate deflection

If the substrate deflects rapidly compared to the rate of capillary rise, the energy made available by immersing the particle to deflect the substrate can be estimated by considering the energy between an initial state of a particle sitting in a planar interface of uniform thickness $\hat{h}_\infty = 0.1$ with contact angle 70° (a configuration that is not in equilibrium) and a final state of a planar interface with film thickness 1.34 in equilibrium with the contact angle θ . The energy difference between these two states can be found using [19] to be $\Delta\alpha = -1.75$. The effects of line tension can be estimated by allowing Σ to alter the initial value for θ_0 according to the modified Young equation, and considering the free energy to cross a planar interface. This analysis has been presented in Fig. 7 of Aveyard and Clint [12], who consider a range of Σ values and who also comment on the free energy activation barriers.

3.4. Bending of flexible membranes by particles

Particles placed in thin liquid films above pulmonary epithelial cell layers have been observed to deflect the cells beneath them. The constitutive response of the cellular layer must be known to determine whether the energy provided by

immersing the particle can perform the work needed to bend the cellular layer. The simplest estimate of the work W required to deflect a membrane can be obtained by considering the product of a membrane tension τ (of typical magnitude on the order of 1–10 mN/m for lipid bilayers [21]) times the expansion area of the cells required to embed the particle in them, which is comparable to the surface area of the particles,

$$W \approx \tau 4\pi a^2, \quad (20)$$

while the energy liberated by immersing the particles is given by:

$$\Delta A^* \approx \Delta\alpha\gamma\pi a^2, \quad (21)$$

where $\Delta\alpha$ is the energy liberated in dimensionless form, discussed above. If the work required to deflect the membrane is comparable to ΔA^* , the particles can deform the cellular layer. Therefore, the ratio $W/\Delta A^* \approx 4\tau/\Delta\alpha\gamma < 1$ (independent of particle radius) determines whether the particles will bend the membranes beneath them to embed themselves. This framework can be readily extended to more complex constitutive relationships to describe the mechanical response of the substrate, which would simply alter the expression for the work W .

4. Conclusions

Analytical expressions for the equilibrium configuration of a particle in a thin liquid film on a solid substrate are found, including the shape of the free surface and the magnitude of the force exerted by the particle on the underlying substrate. The effects of line tension in changing the location of the three-phase contact line are also found. A new dewetting transition is reported at a critical value for the line tension, at which the particle dewets and rests atop the fluid interface rather than immerse itself in the film. For flexible substrates, the downward force created by the wetting

meniscus on the particle can deflect the substrate. Estimates for the energy provided by wetting the particle to bend the surface are provided, including the effects of line tension.

References

- [1] C.W. Nutt, Chem. Eng. Sci. 12 (1960) 183.
- [2] A. Scheludko, B.V. Toshev, D.T. Bojadjiev, J.C.S. Faraday 1 72 (1976) 2814.
- [3] D.Y.C. Chan, J.D. Henry, L.R. White, J. Colloid Interface Sci. 79 (1981) 410.
- [4] B.P. Binks, J.H. Clint, Langmuir 18 (2002) 1270.
- [5] B.P. Binks, S.O. Lumsdon, Langmuir 16 (2000) 8622.
- [6] P. Gehr, S. Schürch, Y. Berthiaume, V. Im Hof, M. Geiser, J. Aerosol Med. 3 (1990) 27.
- [7] D.A. Edwards, J. Hanes, G. Caponetti, J. Hrkach, A. Ben-Jebria, M. Low Eskew, J. Mintzes, D. Dearer, N. Lotan, R. Langer, Science 276 (1997) 1868.
- [8] A.V. Rapacchietta, A.W. Neumann, J. Colloid Interface Sci. 59 (1977) 555.
- [9] C. Huh, L.E. Scriven, J. Colloid Interface Sci. 30 (1969) 323.
- [10] V.N. Paunov, et al., J. Colloid Interface Sci. 157 (1993) 100.
- [11] R. Aveyard, J.H. Clint, J. Chem. Soc. Faraday Trans. 92 (1996) 85.
- [12] R. Aveyard, B.D. Beake, J.H. Clint, J. Chem. Soc. Faraday Trans. 92 (1996) 4271.
- [13] S.M. Patrick, et al., Ann. Biomed. Eng. 29 (2001) 1.
- [14] N.D. Denkov, O.D. Velev, P.A. Kralchevsky, I.B. Ivanov, H. Yoshimura, K. Nagayama, Nature 361 (1993) 26.
- [15] P.A. Kralchevsky, K. Nagayama, Langmuir 10 (1994) 23.
- [16] P.A. Kralchevsky, K. Nagayama, Adv. Colloid Interface Sci. 85 (2000) 145.
- [17] P.A. Kralchevsky, N.D. Denkov, Curr. Opin. Colloid Interface Sci. 6 (2001) 383.
- [18] K.D. Danov, B. Pouligny, P.A. Kralchevsky, Langmuir 17 (2001) 6599.
- [19] M. Abramowitz, I.A. Stegun, Handbook of Mathematical Functions with Formulas, Graphs and Mathematical Tables, Dover, New York, 1972, p. 379.
- [20] J. Mingins, A. Scheludko, J. Chem. Soc. Faraday Trans. 1 75 (1979) 1.
- [21] D. Needham, R.M. Hochmuth, Biophys. J. 55 (1989) 1001.